Adenovirus-mediated small interfering RNA against matrix metalloproteinase-2 suppresses tumor growth and lung metastasis in mice

Chandramu Chetty,[1] Praveen Bhoopathi,[1] Pushpa Joseph,[2] Subramanyam Chittivelu,[3] Jasti S. Rao,[1,4] and Sajani Lakka[1]

Departments of [1]Cancer Biology and Pharmacology, [2]Pathology, [3]Medicine, and [4]Neurosurgery, University of Illinois College of Medicine at Peoria, Peoria, Illinois

Abstract

Matrix metalloproteinases (MMP) are a group of proteinases that have normal physiologic roles degrading and remodeling the extracellular matrix. They also have multiple roles in different stages of tumor progression. Elevated levels of MMPs have been observed in many tumors; these increases have a strong association with the invasive phenotype. MMP-2 and MMP-9 are particularly involved in cancer invasion and metastasis. MMP inhibitors are currently being tested as therapeutic agents for a number of cancers in both preclinical models and in clinical trials. To date, clinical trials using this strategy have had limited efficacy. A major concern is the lack of specificity of commercially available MMP inhibitors. An adenoviral vector expressing small interfering RNA against the *MMP-2* gene (Ad-MMP-2) was constructed to specifically inhibit MMP-2 expression. The effect of Ad-MMP-2 on invasion, angiogenesis, tumor growth, and metastasis of A549 lung cancer cell was evaluated. Ad-MMP-2 infection of lung cancer cells showed specific down-regulation of MMP-2 protein, activity, and transcription as determined by Western blotting, gelatin zymography, and reverse transcription-PCR. Ad-MMP-2 inhibition also mitigated lung cancer invasion and migration, and reduced tumor cell–induced angiogenesis *in vitro*. In an experimental metastatic lung tumor model, treatment of established tumors by Ad-MMP-2 inhibited s.c. tumor growth and formation of lung nodules in mice. Adenoviral-mediated RNA interference against MMP-2 has significant therapeutic potential for lung cancer and exerts some of this effect by inhibiting angiogenesis. [Mol Cancer Ther 2006;5(9):2289–99]

Received 3/28/06; revised 6/23/06; accepted 7/11/06.

Grant support: American Cancer Society (S. Lakka).

The costs of publication of this article were defrayed in part by the payment of page charges. This article must therefore be hereby marked advertisement in accordance with 18 U.S.C. Section 1734 solely to indicate this fact.

Requests for reprints: Sajani Lakka, Program of Cancer Biology, Department of Cancer Biology and Pharmacology, University of Illinois College of Medicine at Peoria, One Illini Drive, Peoria, IL 61605. Phone: 309-671-3445; Fax: 309-671-3442. E-mail: slakka@uic.edu

doi:10.1158/1535-7163.MCT-06-0169

Introduction

Metastatic cancer of the lung is a particularly challenging problem in the clinical setting. Once tumors have invaded the lung, the response to classic chemotherapeutic agents is weak, and the prognosis for these patients is poor (1). Metastasis is a complex, multistep process during which tumor cells spread from the primary tumor mass to distant organs. The metastasis cascade is thought to consist of the following steps: local invasion, intravasation into the systemic circulation, survival during the transport, extravasation and establishment of micrometastases in distant organs, and colonization of macroscopic metastases. To escape from the primary tumor and invade the interstitial extracellular matrix, cells create localized defects in the extracellular matrix using a variety of proteases. Matrix metalloproteinases (MMP) are overexpressed in a variety of malignant tumor types, and their overexpression is associated with tumor aggressiveness and metastatic potential (2). Extracellular matrix degradation by MMPs not only facilitates metastasis but also promotes tumor growth by increasing the bioavailability of growth factors that reside in the extracellular matrix (3, 4). Thus, the control of matrix proteolysis has long been proposed as a rational antitumor therapeutic strategy (5, 6).

MMPs are secreted, zinc-containing metalloenzymes with a high degree of specificity for degrading extracellular matrix components. MMPs are divided into five major subclasses: collagenases, gelatinases (also called type IV collagenases), stromelysins, matrilysins, and membrane-type MMPs. Two types of gelatinases, A and B (MMP-2 and MMP-9, respectively), have been isolated and characterized. Type IV collagen is a major structural protein of basement membranes, including the blood vessel basement membrane, and it is chemically and genetically distinct from stroma collagen types I and III and cartilage collagen type II. In addition, its degradation plays an important role in tumor cell invasion of the vasculature. As a result, MMP-2 and MMP-9 are considered to play essential roles in metastasis. MMP-2 expression has been associated with the invasive potential of cancer cell lines *in vitro* (7). MMP-2 activation has been directly correlated with the aggressiveness of tumor cells (8, 9). Its expression and activity is related to the invasiveness and metastatic potential of various cancer cells (10, 11). Higher levels of MMP-2 have been shown in more invasive and metastatic tumors, giving an inverse prognostic effect in lung cancer (12, 13). Like other MMPs, MMP-2 is secreted as a latent pro-enzyme, pro-MMP-2 (68 kDa pro–gelatinase A), and is processed into its active form, active MMP-2 (62 kDa gelatinase A; ref. 14). It has recently been established that MMP-2 is activated by membrane type 1 MMP on the cell surface (15).

In non–small cell lung cancer, increased MMP-2 has been shown to be associated with an increased propensity for both nodal and distant metastases, whereas increased MMP-2 in serum is correlated with increased metastatic spread and resistance to chemotherapy (16). MMP-2 activation promotes cell viability and secondary growth in metastatic sites *in vivo* (17). Host-derived gelatinase A plays an important role in angiogenesis and tumor progression, suggesting the usefulness of gelatinase A inhibitors for anticancer treatment (18).

A number of MMP inhibitors are being developed for the treatment of cancer. Studies of MMP inhibitor treatments in lung cancer suggest that although side effects are usually tolerable, these drugs do not have any major beneficial effects (19, 20). In the absence of highly specific and effective MMP inhibitors, alternative mechanisms to block gelatinase activity are needed. These results indicate the need for a novel approach for designing new types of MMP inhibitors.

MMP expression and activation involve multiple steps—transcription of MMP genes, secretion of the zymogen into the extracellular matrix, and activation of the zymogen—several of which are amenable for therapeutic intervention. In the present study, we have used an RNA interference (RNAi) approach to inhibit MMP-2 expression. RNAi induced by small interfering RNA (siRNA) has recently emerged as a powerful technique capable of suppressing expression of individual genes with a high degree of specificity. siRNA oligonucleotides have advantages over DNA oligonucleotides in terms of their resistance to nucleases (21) and RNAi seems to have greater potency than antisense-based approaches (22). Plasmid and viral vectors producing siRNA using the polymerase III promoter offer more efficient siRNA delivery and are showing promise both *in vitro* and *in vivo* (23). In the present study, we have constructed an adenovirus carrying a siRNA sequence targeting *MMP-2* gene. Our results confirm that adenoviral-mediated siRNA against MMP-2 down-regulate invasion and show that tumor-derived angiogenesis is reduced *in vitro* and *in vivo*. In addition, i.v. delivery of adenovirus-mediated MMP-2 siRNA gene transfer prevents A549 carcinoma cells from spontaneously metastasizing to the lungs.

Materials and Methods

siRNA Design and Transient Transfection. MMP-2 siRNA sequences were designed with the help of siRNA designer program (Imgenex, Sorrento Valley, CA). The siRNA was complementary to an exonic sequence of the target mRNA and compatible with the pSuppressor plasmid (Imgenex). Four siRNA sequences were cloned in the pSuppressor vector. The following siRNA sequences—(*a*) 5′-AGAGTTGGCAGTGCAATACCT**ATCGATA**GGTATTGCACTGCCAACTCT, (*b*) 5′-CAAATATGAGAGCTGCACCAG**ATCGAT**CTGGTGCAGCTCTCATATTTG, (*c*) 5′-AACGGACAAAGAGTTGGCAGT**ATCGAT**ACTGCCCAACTCTTTGTCCGTT, and (*d*) 5′-CCAAAGTCTGAAGAGCGTGAA**ATCGAT**TTCACGCTCTTCAGACTTTGG—were used to construct the four constructs, pSup-1 to pSup-4, respectively. A control vector containing siRNA with a scrambled MMP-2 sequence was constructed and designated as pSV. The scrambled sequence used is 5′-GCACGGAGGTTGCAAAGAATAATCGATTATTCTTTGCAACCTCCGTGC. A549 lung cancer cells were transiently transfected with these constructs to determine their effect on MMP-2 expression. Briefly, 150,000 cells were seeded in a 6-cm-diameter dish and grown in RPMI 1640 supplemented with 10% FCS. The cells were transfected with 1 μg of the plasmids. LipofectAMINE reagent (Invitrogen, Gaithersburg, MD; 3 μL per transfection) was used according to the instructions of the manufacturer. Following transfection, the cells were cultured in RPMI 1640-10% FCS for 24 hours, rinsed once with PBS, and cultured for additional 16 hours in serum-free DMEM. The conditioned medium was collected and MMP-2 levels were determined by gelatin zymography.

Recombinant Adenovirus Construction. The adenovirus was constructed using adenoviral pSuppressor kit (Imgenex) per instructions of the manufacturer. The pSuppressor plasmid (pSup-3) containing the MMP-2 siRNA sequence 5′-AACGGACAAAGAGTTGGCAGT**ATCGAT**ACTGCCCAACTCTTTGTCCGTT-3′ were digested with *Pac*I and cotransfected with pAd vector backbone in 293 cells for the generation of adenovirus containing MMP-2 siRNA (Ad-MMP-2). The pSV construct was used to construct adenovirus containing the scrambled sequence, Ad-SV. Adenovirus generation, amplification, and titer were done according to previously described procedures (24). Viruses were plaque purified, propagated on 293 cells, and purified by cesium chloride gradient according to standard techniques. Particle titers of all adenoviruses were determined by absorbance measurements at 260 nm, and functional titers (plaque-forming units) were determined by end-point dilution titration on 293 cells according to standard techniques. The amount of infective adenoviral vector per cell (plaque-forming units/cell) in culture medium was expressed as multiplicity of infection (MOI).

Cell Proliferation Assay (3-(4,5-Dimethylthiazol-2-yl)-2,5-Diphenyltetrazolium Bromide Assay). Ten thousand cells per well of a 96-well tissue culture dish were plated and infected with mock (PBS), 50 MOI of Ad-SV, or the indicated MOI of Ad-MMP-2 virus in triplicate. The proliferation rate at 24, 48, and 72 hours was determined with a 3-(4,5-dimethylthiazol-2-yl)-2,5-diphenyltetrazolium bromide assay (Chemicon International, Temecula, CA). The assay was optimized to verify that the signal obtained was within the linear range for the reagent. Absorbance of the medium was measured at 570 nm.

Gelatin Zymography. MMP activity in conditioned medium was determined by gelatinase zymography as we described previously (25). A549 cells were infected with mock, Ad-SV, and the indicated doses of Ad-MMP-2 for 36 hours. The cells were washed and incubated with serum-free medium overnight. Conditioned medium containing equal amounts of protein were electrophoresed in

7.5% SDS-polyacrylamide gels containing 1.5 mg/mL gelatin. The gels were washed and gently shaken in three consecutive washings in 2.5% Triton X-100 solution to remove SDS. The gels were then incubated at 37°C overnight in incubation buffer [50 mmol/L Tris-HCl (pH 7.5), 0.05% NaN_3, 5 mmol/L $CaCl_2$, and 1 μmol/L $ZnCl_2$]. The gel was stained with 0.1% Coomassie brilliant blue in 10% acetic acid and 10% isopropanol and subsequently destained for 1 hour. Gelatinolytic activities were identified as clear zones of lysis against a blue background.

Immunofluorescence. Lung cancer cells (5×10^3) were cultured in chamber slides and infected with mock, 50 MOI Ad-SV, or the indicated MOI of Ad-MMP-2 and cultured for 48 hours. At the end of incubation, the cells were fixed in cold, fresh acetone-methanol (1:1) for 15 minutes, and finally permeabilized in PBS/Triton X-100 (0.1%). For blocking, cells were incubated with 3% bovine serum albumin at ambient temperature for 2 hours, followed by staining with 1:100 dilution mouse anti-MMP-2 in PBS (Santa Cruz Biotechnology, Santa Cruz, CA) for 2 hours. Mouse IgG was used as a negative control. The cell preparations were washed at least thrice with PBS-Tween (0.05%) and then incubated with mouse FITC-conjugated secondary antibodies. After washing off the excess reagents with PBS-Tween, the cells were mounted and counterstained in 4′,6-diamidino-2-phenylindole–containing mounting solution (Vector Laboratories, Burlingame, CA) and visualized by fluorescence microscopy imaged with an Olympus camera.

Western Blot Analysis. A549 lung cancer cells were infected with mock, Ad-SV, or the indicated MOI of Ad-MMP-2 for 48 hours. Cell lysates were prepared by lysing cells in radioimmunoprecipitation assay buffer [50 mmol/L Tris-HCl (pH 8.0), 150 mmol/L NaCl, 1% NP40, 0.5% sodium deoxycholate, 0.1% SDS, 0.5 mmol/L phenylmethylsulfonylfluoride] and resolved by SDS-PAGE. Immunoblotting was done on polyvinylidene fluoride membranes (Millipore, Billerica, MA) according to the instructions of the manufacturer. After blocking with 5% nonfat dry milk and 0.1% Tween 20 in TBS, membranes were incubated with 1:1,000 dilution of mouse anti-MMP-2 antibody. The membranes then were developed using anti-mouse peroxidase-labeled secondary antibodies. Protein bands were visualized using the ECL system (Amersham Pharmacia, Piscataway, NJ). Actin protein levels were used as a control to verify equal protein loading.

Reverse Transcription-PCR. Total RNA was extracted using TRIZOL reagent according to the protocol provided by the manufacturer (Life Technologies, Grand Island, NY). RNA thus obtained was further purified by digesting with DNase for 20 minutes at 37°C and then reverse transcribed using the cDNA cycle kit (Invitrogen, Carlsbad, CA) with random primers (26). To amplify the cDNA, the reverse-transcribed cDNA was subjected to 30 cycles of PCR in 25 μL PCR Master Mix (Promega, Madison, WI) containing 100 pmol sense and antisense primers set for denaturation at 94°C for 1 minute, annealing at 55°C for 30 seconds, and extension at 72°C for 90 seconds. The expected PCR products were electrophoresed on 2% agarose gels and were visualized by ethidium bromide staining. To normalize for the amount of input RNA, reverse transcription-PCR was done with primers for the constitutively expressed *glyceraldehyde-3-phosphate dehydrogenase* gene. The specific primers used in this study were as follows: *MMP-2*, sense 5′-GTGCTGAAGGACACACTAA AGAAGA-3′ and antisense 5′-TTGCCATCCTTCTCAAAGTTGTAGG-3′; *glyceraldehyde-3-phosphate dehydrogenase*, sense 5′-TGAAGGTCGGAGTCAACGGATTTGGT-3′ and antisense 5′-CATGTGGGCCATGA GGTCCACCAC-3′. *OAS1*, sense 5′-AGGTGGTAAAGGGTGGCTCC-3′ and antisense 5′-ACAACCAGGTCAGCGTCAGAT-3′. To determine the quantity of PCR products on the agarose gel, focus images were generated by Alpha Innotech Image Acquisition and Analysis Software, and images were processed for display using Adobe Photoshop 6.0 (Adobe, Mountain View, CA). Quantification of *MMP-2* gene expression was based on densitometry readings. Statistical analysis was done to calculate the gel intensity using Microsoft Excel software.

Spheroid Migration Assay. Two-dimensional spheroid outgrowth assays were done as described before (27). Tumor spheroids were prepared by plating A549 cells in 96-well, low-attachment plates. Cells (5×10^4 per well) were plated and cultured on a shaker at 100 rpm at 37°C for 2 to 4 days to form single spheroids. A single spheroid was removed and trypsinized to determine the cell number. The spheroids were transferred to eight-well chamber slides and infected with mock, Ad-SV, or the indicated MOI of Ad-MMP-2 for 48 hours. Following a 48-hour incubation period, the radial distance of migration was measured using Image Pro Discovery software.

***In vitro* Invasion**. A bioassay for *in vitro* cell invasion using Matrigel Invasion Chambers (Fisher Scientific, Pittsburgh, PA) was done as described previously (27). A549 lung cancer cells were infected with mock, 50 MOI of Ad-SV, or the indicated MOI of Ad-MMP-2. After a 24-hour incubation period, the cells were trypsinized and 1×10^6 cells were placed in transwell inserts coated with Matrigel (0.7 mg/mL). Following 24 hours of incubation at 37°C in a humidified 5% CO_2 atmosphere, cells in the upper chamber and on the Matrigel were mechanically removed with a cotton swab. Cells adherent to the outer surface of the membrane were fixed in 25% methanol and stained with crystal violet. The invading cells were counted and photographed under a microscope (FluoView) at ×20 magnification. Five fields were counted per filter in each group; the experiment was conducted in triplicate and repeated on three occasions.

***In vitro* Microtubule Network Formation Assay.** Tumor cell conditioned medium–induced microtubule network formation was determined as described previously (28). Human microvascular endothelial cells C (5×10^3/0.2 mL) were plated in eight-well chamber slides and were incubated at 37°C for 8 hours. The medium was removed and replaced with 0.2 mL conditioned medium from A549 cells infected with PBS (mock), 50 MOI of Ad-SV, and 25 and 50 MOI of Ad-MMP-2 virus. The medium was replaced every 24 hours and the cell were cultured for

72 hours. At the end of incubation, each well was washed in PBS, fixed with 0.2 mL of 100% methanol for 20 minutes, and stained with 0.25% crystal violet solution. The formation of the microtubule networks were examined by using a phase-contrast microscope equipped with an Olympus camera and evaluated by Discover Image pro software. All experiments were repeated at least twice. Results are presented as the means ± SD of eight fields.

Ad-MMP-2 Gene Therapy for the Experimental Metastasis Lung Model in Mice

Animal Experiments. The pulmonary metastasis model of A549 human lung carcinoma cells in SCID mice was established as described previously (27) and was used to assess the therapeutic effects of Ad-MMP-2. Briefly, parental A549 cells were grown to 80% to 90% confluence in 100-mm dishes and were harvested by trypsin-EDTA. The cells were washed twice with serum-free medium and resuspended in PBS at a concentration of 5×10^7/mL. Cells (5×10^6/0.1 mL) were grafted into flank of 6-week-old female SCID mice. When the mean tumor diameter reached 3 to 4 mm (around 12–14 days), the mice were separated into three groups with five animals per group. Each group was injected i.v. with PBS (mock) or 5×10^8 plaque-forming units of either Ad-SV or Ad-MMP-2 virus thrice with 3-day intervals. Animals were then maintained to allow further growth of lung metastasis for an additional 5 weeks. S.c. tumor growth was measured every week with vernier calipers and tumor volume was calculated using the formula 0.5 ($R_{max} \times R_{min}^2$). The regression in the s.c. tumor growth was followed for up to 5 weeks. Mice were euthanized when the tumor diameter in control mice measured between 1.2 and 1.1 cm; s.c. tumors and lungs were removed and fixed; and visible lung metastases were counted in fixed tissues. S.c. tumor and lung sections were stained with H&E. For MMP-2 or vessel staining, the sections were first deparaffinized in xylene and rehydration through graded ethanol. Antigen retrieval was done by microwave heating sections in 10 mmol/L sodium citrate buffer (pH 6) for 10 minutes. Following quenching of endogenous peroxidase activity and blocking of nonspecific binding, sections were incubated with an anti-MMP-2 monoclonal antibody (Calbiochem, San Diego, CA) or CD31 (endothelial surface marker) monoclonal antibody (Biomeda, Foster City, CA) at 4°C overnight at a 1:200 dilution. The secondary antibody was biotinylated rabbit anti-mouse antibody (DAKO, Carpinteria, CA) used at a dilution of 1:200 for 30 minutes at 37°C. After further washing with TBS, sections were incubated with StrepABComplex/horseradish peroxidase (1:100; DAKO) for 30 minutes at 37°C. Immunolocalization was done by exposure to 0.05% 3,3′-diaminobenzidine tetrahydrochloride as the chromogen. Serum was used in the place of primary antibody as a negative control. The slides were counterstained with Mayer's hematoxylin, dehydrated, and mounted with aqueous, antifading mounting medium (Biomeda). All microscopy studies were done with an Olympus microscope [WH10×-H/22 eyepiece with a high-power field (×20) area of 0.16 mm^2] set to auto.

Statistical Analysis. Data from *in vitro* experiments are presented as means ± SD. Statistical significance between treatment groups and controls in their tumor growth rates was estimated by the two-tailed nonparametric Mann-Whitney test.

Results

Construction of Ad-MMP-2 siRNA

We constructed two adenoviral vectors: one contains the siRNA sequence of *MMP-2* gene (Ad-MMP-2) and the other contains the scrambled sequence. We initially selected four sequences using the Imgenex siRNA designer program, and these sequences were homologous only to MMP-2 mRNA as confirmed with National Center for Biotechnology Information Blast search engine. These four sequences were cloned hybridized and inserted into the pSuppressor vector under control of modified Pol II promoter (Imgenex) for quick screening of the recombinant plasmids. We transfected these four (pSup-1-4) constructs in A549 lung cancer cells and determined the MMP-2 levels (Fig. 1A). The plasmid that exhibited the maximum inhibition of MMP-2 expression (pSup-3) was used to construct the experimental adenovirus (Ad-MMP-2). We also constructed a control adenovirus, which contained the scrambled sequence of this MMP-2 siRNA (Ad-SV).

Ad-MMP-2 Inhibits Endogenous MMP-2 Expression in Cancer Cells

To test the efficacy of the adenoviral-mediated delivery of the selected siRNA sequence, we infected A549 with Ad-MMP-2 and Ad-SV. MMP-2 activity in the conditioned medium was examined using gelatin zymography. Zymographic analysis revealed bands of an estimated molecular weight of 72 kDa. MMP-2 activity was more intense in cells treated with PBS (mock) and scrambled vector (Ad-SV). There was a dose-dependent inhibition of MMP-2 activity in cells infected with increasing concentrations of Ad-MMP-2 (Fig. 1B). Western blot analysis and immunocytochemistry were done to confirm gelatinolytic results using specific antibodies for MMP-2. Proteins from the cell extracts were immunoblotted with monoclonal antibodies specific for MMP-2. Western blot analysis using a MMP-2 antibody showed a band of 72 kDa in the cell lysates. Significant bands were detected from cells infected with PBS (mock) and Ad-SV. Cell lysates from cells treated with 25 MOI of Ad-MMP-2 showed a remarkable decrease in MMP-2 expression levels and 50 MOI of Ad-MMP-2 showed barely detectable 72 kDa bands (Fig. 1C). Immunocytochemical analysis of cells infected with Ad-MMP-2 and Ad-SV revealed reduced signals in Ad-MMP-2–infected cells (Fig. 1D). To determine whether decreased production of MMP-2 was caused by gene transcription, we examined the levels of MMP-2 transcripts using reverse transcription-PCR. As shown in Fig. 1E, the abundance of MMP-2 transcripts in Ad-MMP-2–infected cells were significantly lower compared with cells infected with mock and Ad-SV. Under certain conditions, siRNA may also activate components of the IFN system, potentially affecting gene

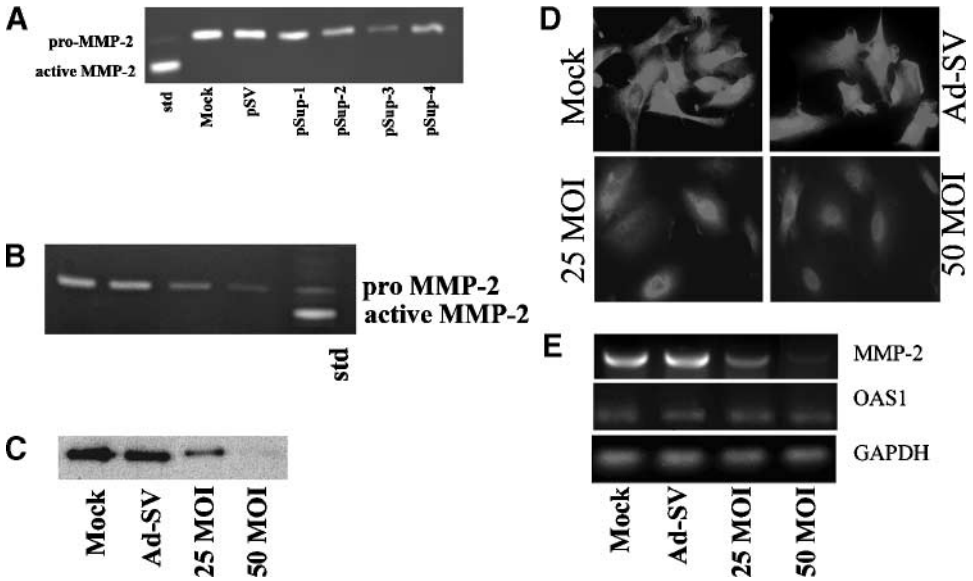

Figure 1. Ad-MMP-2 infection inhibits MMP-2 activity, and protein and mRNA levels. **A,** gelatin zymographic analysis of A549 cells transiently infected with the four siRNA constructs. **B,** zymographic analysis for MMP-2 activity in the conditioned medium of cells infected with mock (PBS), 50 MOI of Ad-SV, and 25 and 50 MOI of Ad-MMP-2. **C,** Western blot analysis of MMP-2 protein expression in the lysates of cells infected with mock (PBS), 50 MOI of Ad-SV, and 25 and 50 MOI of Ad-MMP-2. **D,** immunocytochemistry for MMP-2 expression in A549 cell showing intense staining in cells infected with mock and 50 MOI of Ad-SV than cells infected with the indicated MOI of Ad-MMP-2. **E,** reverse transcription-PCR analysis showing reduced MMP-2 mRNA expression in control and Ad-SV – infected cells. Total RNA was extracted as per standard protocols from A549 cells infected with mock, 50 MOI of Ad-SV, and 25 and 50 MOI of Ad-MMP-2, and cDNA was synthesized as described in Materials and Methods. The PCR reaction was set up using the first-stand cDNA as the template for MMP-2 and OAS1. Glyceraldehyde-3-phosphate dehydrogenase (*GAPDH*) served as a loading control. The experiments were repeated thrice.

expression (29, 30). However, not all of the silencing vectors or synthetic siRNAs tested caused this effect, suggesting that the ability to induce the IFN system depends on some aspect of both the siRNA sequence and its method of delivery. We have determined the expression of *OAS1*, one of the IFN-stimulated gene in A549 cells infected with mock, Ad-SV, or Ad-MMP-2 (25 and 50 MOI). We did not detect any increase in the expression of *OAS1*, suggesting that MMP-2 inhibition by Ad-MMP-2 is a specific response to siRNA-mediated targeting of MMP-2 (Fig. 1D).

In vitro Growth of Ad-MMP-2–Infected Cells

To determine whether MMP-2 inhibition effected the growth of A549 cells, the growth rates of cells infected with Ad-MMP-2 were compared with that of the parental and Ad-SV–infected controls. No significant differences in growth rate were observed between MMP-2–inhibited and control cells up to 48 hours (Fig. 2).

Ad-MMP-2 Infection Inhibits Tumor Cell Migration

Cleavage of extracellular matrix components is a key requirement for cell migration, and proteolysis releases growth factors and other signaling molecules from extracellular stores. To evaluate the effects of MMP-2 inhibition on tumor cell migration, we compared the migration of Ad-MMP-2–infected A549 tumor cell spheroids with that of the mock and Ad-SV–infected controls in a two-dimensional tumor spheroid. There was significant radial migration of the cells from mock and Ad-SV–infected spheroids. The outgrowth of cells was significantly inhibited in spheroids infected with Ad-MMP-2 virus (Fig. 3A). There was dose-dependent inhibition of migration of Ad-MMP-2–infected A549 tumor cell spheroid compared with control groups as determined by Image Pro analysis (Fig. 3B).

Effect of Ad-MMP-2 on Lung Cancer Cell Invasion

Because the action of matrix-degrading proteinase is a critical component of cellular invasion, the effects of Ad-MMP-2 on invasion were determined *in vitro*. We observed

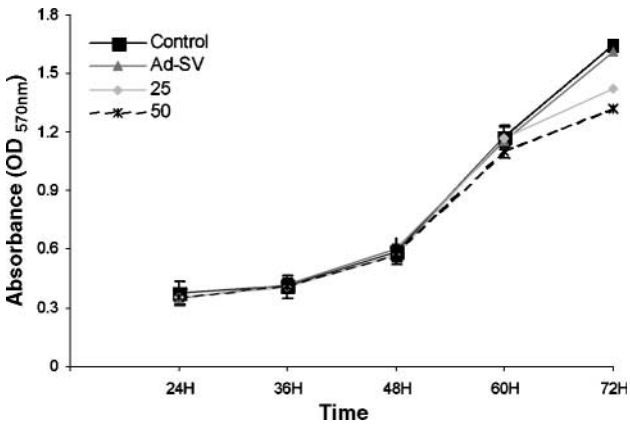

Figure 2. Effect of Ad-MMP-2 on A549 cell proliferation as determined by 3-(4,5-dimethylthiazol-2-yl)-2,5-diphenyltetrazolium bromide assay. A549 cells were infected with mock, 50 MOI of Ad-SV, and 25 and 50 MOI of Ad-MMP-2 virus. Absorbance was recorded at 570 nm. Values were plotted after subtracting the blank absorbance (*OD*). *Points,* means of three experiments; *bars,* SD.

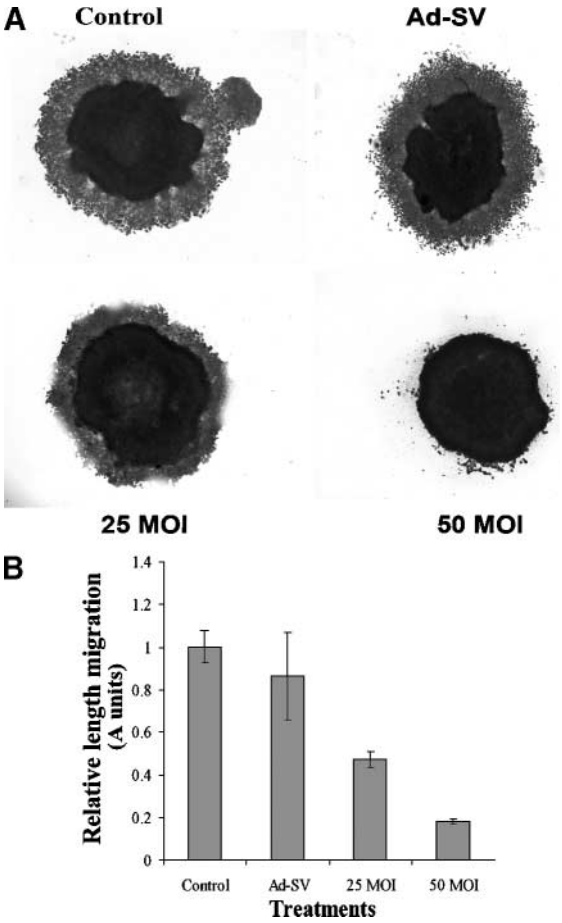

Figure 3. Ad-MMP-2 infection inhibits lung cancer cell migration. A549 cells were seeded onto low attachment plates and cultured until spheroids were formed as described in Materials and Methods. Spheroids were transfected with mock, 50 MOI of Ad-SV, and 25 and 50 MOI of Ad-MMP-2, and cultured at 37°C for 48 h. **A,** at the end of the migration assay, spheroids were fixed with 0.25% crystal violet solution and photographed. **B,** the distance of migration from the center of the spheroid was quantified using Image Pro software. Representative of three independent experiments.

a dose-dependent inhibition of invasion of A549 cells through Boyden chambers coated with Matrigel (Fig. 4A). To facilitate the comparison of the relative invasiveness between controls and Ad-MMP-2–infected cells, all values were normalized to the percentage invasion of control cells, which was taken as 100% (Fig. 4B). The results showed that 25 and 50 MOI of Ad-MMP-2 inhibited invasion by 40% to 50% and 90%, respectively, compared with mock and scrambled vector controls.

Ad-MMP-2 Inhibits Endothelial Network Formation *In vitro*

Matrix proteolysis is thought to play a crucial role in several stages of tumor progression, including angiogenesis and the invasion and metastasis of tumor cells. We next asked whether the inhibition of MMP-2 could influence tumor cell–induced microtubule network formation by endothelial cells. Human microvascular endothelial cells were cultured in the presence of conditioned medium from A549 lung cancer cells infected with mock, 50 MOI of Ad-SV, and various doses of Ad-MMP-2. Very distinct microtubule networks were visualized after H&E staining of endothelial cells cultured in the presence of conditioned medium from mock and Ad-SV–infected lung cancer cells. Conditioned medium from lung cancer cells infected with Ad-MMP-2 significantly reduced the induction of network formation in endothelial cells in a dose-dependent manner (Fig. 5A). Two angiogenic variables, microtubule length per field (Fig. 5B) and branch points per field (number of microtubules; Fig. 5C), were considered as measures of *in vitro* microtubule-like network formation. Image analysis indicated that Ad-MMP-2 treatment decreased the length of microtubule as well as the number of branch points in a dose-dependent manner compared with control groups.

Significant Reduction of Experimental Tumor Metastasis after Treatment with Ad-MMP-2

The therapeutic effects of Ad-MMP-2 were assessed in an experimental model, which assayed the degree to which s.c. injected A549 cells were able to induce lung nodule formation. In this model, established A549 s.c. xenografts were treated (i.v., via the tail vein) with a total dose of 5×10^8 plaque-forming units Ad-SV or Ad-MMP-2 or with the same volume of PBS. Treatment with Ad-MMP-2 significantly suppressed s.c. tumor growth compared with the PBS controls (Fig. 6). There was no difference in the s.c. growth between the mice that received PBS or Ad-SV injections. Mice that received PBS and Ad-SV showed an increase in tumor volume, whereas the mice that received the active Ad-MMP-2 construct exhibited a 60% reduction in tumor volume. H&E staining of the s.c. tumors removed from the treatment group showed very frequent and wide necrotic regions exhibiting increased eosinophilia with nuclear karyorrhexis and karyolysis, whereas the control tumors had very minimal necrosis (Fig. 7A).

Metastasis occurred in 100% of the PBS-treated and Ad-SV control animals. Tumor volume in mice treated with mock, Ad-SV, and Ad-MMP-2 are 1,620 ± 54, 1,670 ± 37, and 420 ± 18, respectively. Metastatic nodules, >2 mm in diameter, were counted and the mean number of nodules in mock and Ad-SV treatments was 15 ± 3 and 14 ± 4, respectively. We could not detect any nodules on the lungs of the mice that received Ad-MMP-2. Lung tissue sections from all three groups were scanned microscopically for metastatic foci by a pathologist (P.J.) blinded to the treatment conditions. There were no metastatic foci in the lung tissue sections from mice that received Ad-MMP-2 treatment. These results clearly show that the adenoviral delivery of MMP-2 siRNA significantly suppresses metastatic ability, as well as tumor growth rate, in SCID mice.

Expression of both MMP-2 and CD31 Was Diminished in Ad-MMP-2–Treated Mice

MMP-2 expression was analyzed in s.c. tumor tissue (Fig. 7A) and lung tissue sections (Fig. 7B). Sections from mice that received mock and Ad-SV treatments showed large amounts of MMP-2. In contrast, there was a decrease in the staining for MMP-2 in tumors from the

Ad-MMP-2–treated mice. To determine whether the inhibition of MMP-2 affected angiogenesis, the sections were stained with CD31 monoclonal antibody in s.c. tumor tissue (Fig. 7A) and lung tissue sections (Fig. 7B), which allows for the visualization of blood vessels. A significant reduction of stained vessels was observed in the treatment group when compared with the control group.

Discussion

The findings of the present study show the potent therapeutic effect of adenovirus-mediated gene therapy of siRNA against MMP-2 for lung cancer in an experimental metastasis model using SCID mouse. At present, adenovirus is still an attractive vector to deliver antiangiogenic and/or anti-invasive gene products for the treatment of cancer because of its high infectivity *in vivo*, which allows for direct vector injection in the clinic, and avoids additional manipulations *in vitro* as required for other vector systems such as the retrovirus. The most encouraging finding from a preclinical viewpoint is that all of the mice that received i.v. injections of Ad-MMP-2 could inhibit the formation of lung metastasis and regressed s.c. tumor growth.

RNAi was shown as a promising strategy for target-directed therapies in a range of diseases (31–33). A large number of disease-relevant target transcripts have been subjected to RNAi, including genes associated with cancer (e.g., *K-ras*; ref. 23) and viral infections (e.g., HIV-1; ref. 34). RNAi has been induced *in vivo* in adult mice using synthetic siRNAs and short hairpin RNAs expressed from plasmid and viral vectors (35, 36). These studies show sequence-specific silencing in tissues harvested from the injected mice with up to ~80% inhibition of the targeted molecule.

Cancer cell invasion is a complex process that requires coordinated interactions between adhesive proteins and pericellular proteolysis. Several reports indicate a role of MMP-2 in tumor cell invasion. For example, ethanol-stimulated cell invasion was, at least partially, mediated by its effect on MMP-2 activation in mammary epithelial cells (37). MMP-2 antisense suppressed the invasive potential of oral squamous cell carcinoma cells (38). MMP-2 was shown to induce migration of breast epithelial cells by exposing a putative cryptic promigratory site on Ln-5 that triggers cell motility (39). *Caveolin-1* gene suppresses pulmonary metastasis from primary mammary tumors in part due to reduced secretion of the gelatinases MMP-2 and MMP-9 (40). Our results also showed that adenovirus-expressing siRNA against MMP-2 (Ad-MMP-2) infection inhibited MMP-2 protein expression, tumor cell migration, and invasion. There was no significant effect on the viability of the cells infected with Ad-MMP-2 virus (up to 48 hours) as determined by the 3-(4,5-dimethylthiazol-2-yl)-2,5-diphenyltetrazolium bromide assay, thereby indicating that the decrease in MMP-2 activity expression and invasive potential were not due to the cytotoxicity of virus. We tested the efficacy of Ad-MMP-2 treatment using an experimental lung metastasis model. We observed that A549 cells injected s.c. formed s.c. tumor growth and metastasized into lungs in all of the animals. We did not observe metastasis into any other organ. The i.v. injection of Ad-MMP-2 virus resulted in the inhibition of s.c. tumor growth and pulmonary metastasis. Moreover, the s.c. tumors from mice, which received Ad-MMP-2 virus, showed very frequent and wide necrotic regions when compared with control tumors. Inhibition of tumor growth by MMP-2 inhibition has been shown before. For example,

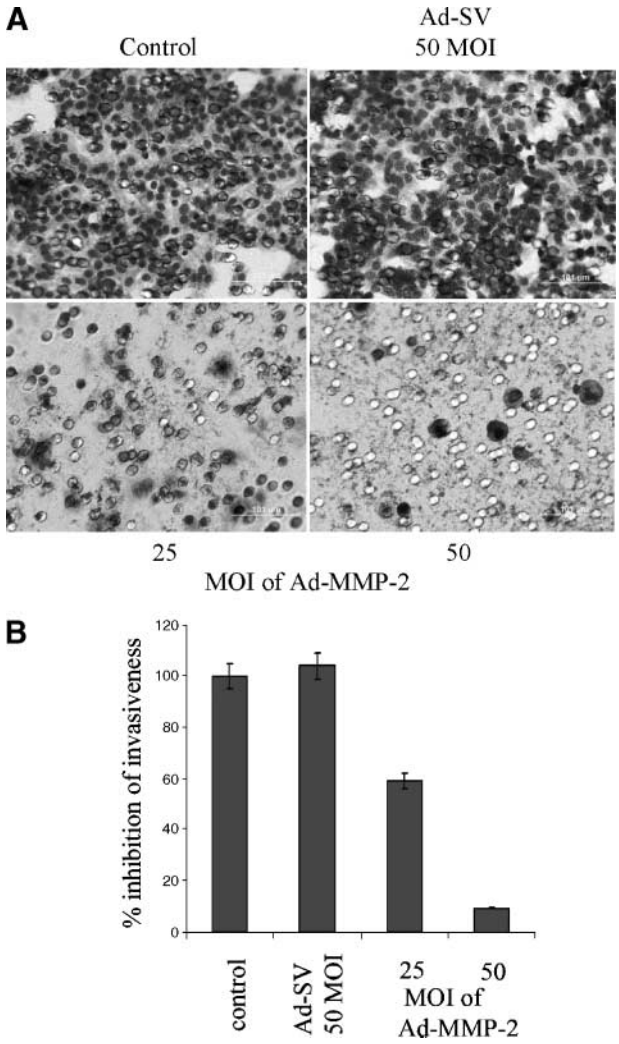

Figure 4. Ad-MMP-2 infection inhibits A549 cancer cell invasion. A549 lung cancer cells were infected with 50 MOI of Ad-SV, 25 and 50 MOI of Ad-MMP-2, and incubated for 24 h. Cells were trypsinized and counted, and 1×10^6 cells in each treatment were allowed to invade transwell inserts containing 12-μm-pore polycarbonate membranes precoated with Matrigel for 24 h at 37°C after which they were fixed and stained with Hema-3. **A,** cells that had migrated to the lower side of the membrane were photographed under a light microscope at ×20 magnification. **B,** percentages of invading cells were quantified by counting five fields in each condition. *Columns,* mean of three separate experiments; *bars,* SD. $P < 0.03$.

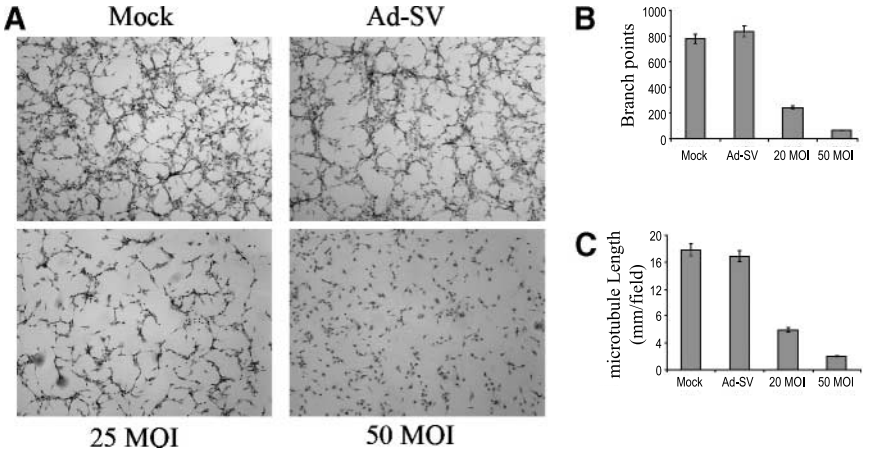

Figure 5. Ad-MMP-2 infection in A549 cells inhibits tumor culture medium–induced microtubule network formation in endothelial cells. Human dermal endothelial cells (4×10^4) were seeded in eight-well chamber slides and cultured with conditioned medium collected from A549 lung cancer cells infected with mock (PBS), 50 MOI of Ad-SV, and 25 and 50 MOI of Ad-MMP-2. **A,** after 72 h, the cells were washed with PBS and stained and photographed. Microtubule length (**B**) and branch points (**C**) were quantitated using Image Pro software. *Columns,* mean of three separate experiments; *bars,* SD.

inhibition of endogenous MMP-2 by an overexpression of tissue inhibitor of metalloproteinase-2 in human melanoma cells resulted in altered cell behavior *in vitro* (41, 42) and reduced tumor growth in mice (43). Inhibition of MMP-2 by Ad-tissue inhibitor of metalloproteinase-1 in CT-26 liver tumor model contributed to antitumor efficacy (44). We believe that the *in vivo* growth inhibitory effect by Ad-MMP-2 in the present study is also partly mediated by inhibition of angiogenesis. Ad-MMP-2 infection of lung cancer cells inhibited their ability to induce tumor cell–induced microtubule network formation in endothelial cells. *In vitro* assays that use matrix proteins and mimic *in vivo* vascularization show accelerated endothelial tube formation when exogenous MMP-2 is added (45). The Ad-MMP-2–treated tumors were less vascularized and tumor apoptosis and/or necrosis could then be related to the hampered tumor angiogenesis, a critical survival condition *in vivo* for nutritional support. In an effort to support this interpretation, we have compared the microvessel densities in the tumors from mice, which received mock, Ad-SV, and Ad-MMP-2 virus and observed decreased microvessel densities in the tumors of mice, which received Ad-MMP-2. Several studies have documented the role of MMP-2 in angiogenesis. Suppression of MMP-2 activity by antisense oligonucleotides in the vascular nodules resulted in the loss of angiogenic potential both *in vitro* and *in vivo* in the chick chorioallantoic membrane assay and this suppression of MMP-2 activity in angiogenic nodules inhibited tumor growth *in vivo* by ~70% (46). In MMP-2–deficient mice, tumor-induced angiogenesis was suppressed according to dorsal air sac assay. The number of lung colonies of i.v. injections fell by 77% for Lewis lung carcinoma in MMP-2–deficient mice (47). These results strongly implicate the activity of MMP-2 as a requirement for tumor progression and angiogenesis.

A large amount of emergent data has confirmed the involvement of a finely regulated balance between MMPs and their inhibitors in a wide range of physiologic processes, from wound repairing to organ/tissue development (48, 49). These findings are in favor of restricting, if possible, MMP inhibition to the tumor site. BMS-275291 is a novel, nonhydroxamate MMP inhibitor, prospectively designed to inhibit a broad spectrum of MMPs that showed more selectivity toward MMP-2 and was well tolerated and less toxic, but phase II trials indicated lack of efficacy with a high rate of disease progression (50). Metastat, or COL-3, is a chemically modified tetracycline that is able to inhibit neutrophil gelatinase and MMP expression in colon, breast, or melanoma cancer models. Randomized phase II trials of this drug in AIDS-related Kaposi's sarcoma patients indicated it to be a promising agent for the treatment of this opportunistic neoplasm of AIDS (51). In this regard, our study shows that i.v. injection of adenovirus-carrying siRNA against MMP-2 was able to restrict the primary s.c. tumor and prevent lung metastasis. In our study, we did not observe any rebound of tumor growth and metastasis in Ad-MMP-2–treated mice. Furthermore, the reduced s.c. tumor growth observed in the Ad-MMP-2–treated mice was mostly necrotic. Several studies have shown that siRNA-directed suppression of a targeted gene *in vivo* was maintained for up to 2 weeks (33, 35). Double-stranded siRNAs were shown to resist biodegradation in FCS and in human plasma (21). The sustained suppression of MMP-2

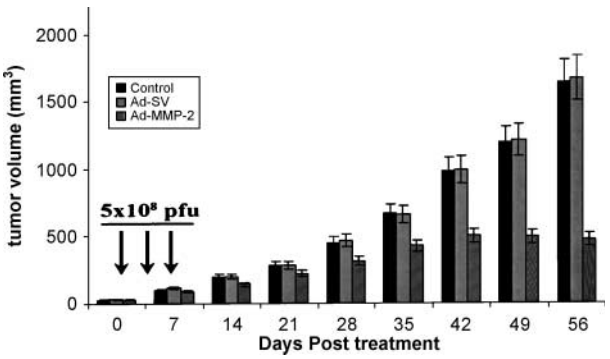

Figure 6. I.v. injection of Ad-MMP-2 virus inhibited s.c. tumor growth in the experimental metastasis model. Mice were treated thrice with PBS, 5×10^8 plaque-forming units of Ad-SV or Ad-Ad-MMP-2 as described in Materials and Methods. *Columns,* mean tumor volumes of five animals per treatment group; *bars,* SD.

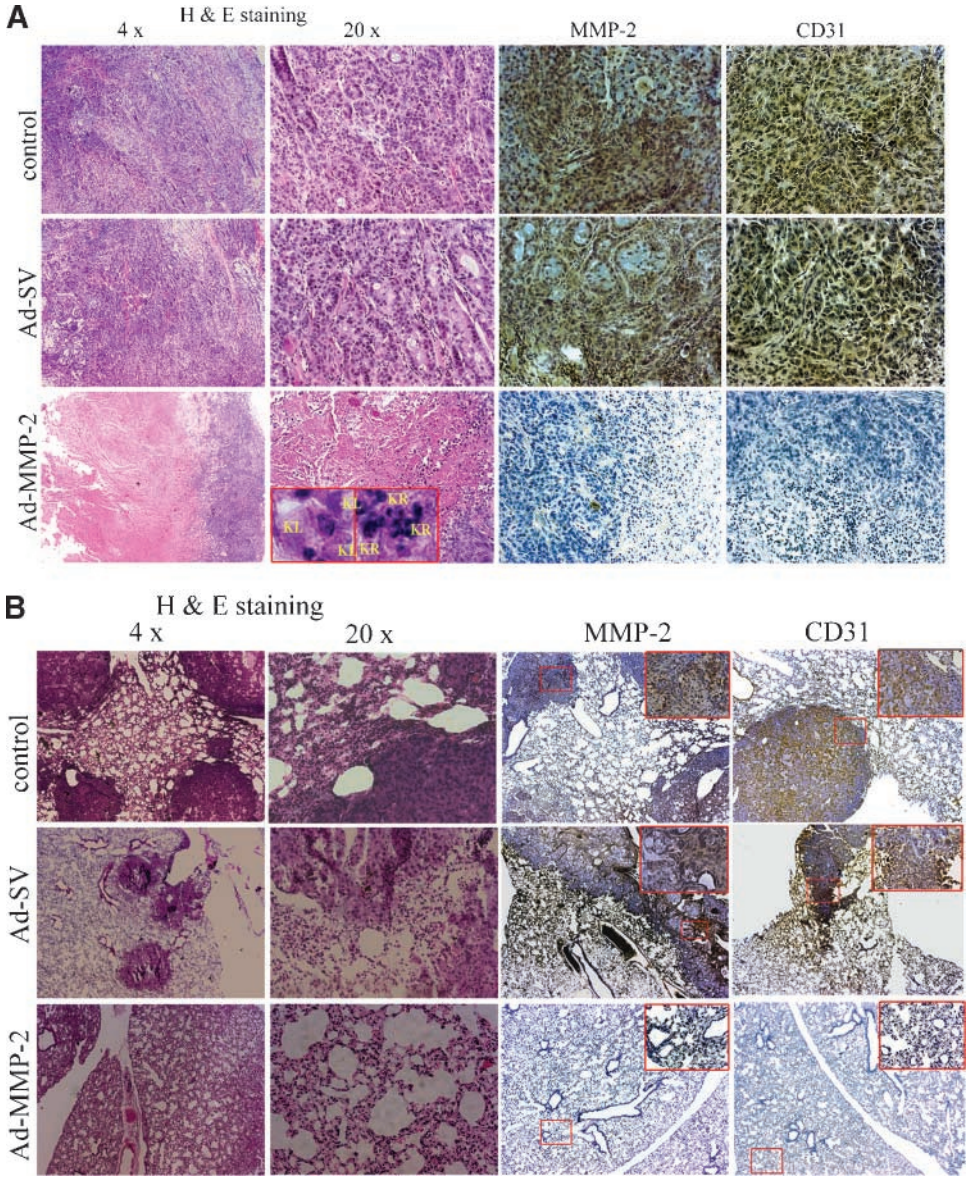

Figure 7. **A,** H&E staining of s.c. tumor showing neoplastic growth. Tumors from Ad-MMP-2–treated mice show extensive necrosis. *Inset,* karyorrhexis (*KH*) and karyolysis (*KL*); magnification, ×60. MMP-2 and CD31 visualized with MMP-2 and CD31 antibodies are significantly inhibited in tumors from mice treated with Ad-MMP-2 compared with mock and Ad-SV controls. **B,** H&E staining of lung sections showing lung nodules in control and Ad-SV–treated mice. Mice that received Ad-MMP-2 did not show any tumor cells in lung sections. There was no detectable MMP-2 and CD31 expression in lung sections from mice treated with Ad-MMP-2 (inset magnification, ×20).

in our study might also be due to siRNA amplification, which occurs in lower species (52). The inherently high permeability of tumor neovasculature (53) could contribute to the activity of systemically administered siRNA. Because silencing after duplex siRNA injection is prolonged but not permanent with adenoviral injection, long-term toxicity is probably of little concern. Further, targeted suppression of a single gene expression would allow therapies to be tailored to the expression profile of an individual patient's tumor.

In summary, our findings confirm that adenoviral-mediated, siRNA-mediated suppression of MMP-2 represents a powerful new approach to understanding the role of these enzymes in lung cancer and provides a potential avenue for new anti-MMP-2 cancer therapies and support further investigation of siRNA as a therapeutic strategy in human lung cancer patients. The use of adenovirus to deliver siRNA to diminish target gene expression in brain and liver tissue *in vivo* has been shown previously (54). One potential problem with the use of an adenoviral vector of the first generation is that it has limited expression of the transgene over time and significant acute toxicity when used at a high dosage (55). We believe that further improvements in vector efficiency and safety, gene expression control systems, and in clinical management of gene delivery routes will allow siRNA-mediated, anti-MMP-2 therapy to progress to a clinical reality.

Acknowledgments

We thank Shellee Abraham for manuscript preparation, Sushma Jasti and Diana Meister for manuscript review, and Noorjehan Ali for her help with the animal experiments.

References

1. Cohen V, Khuri FR. Progress in lung cancer chemoprevention. Cancer Control 2003;10:315 – 24.

2. Kahari VM, Saarialho-Kere U. Matrix metalloproteinases and their inhibitors in tumour growth and invasion. Ann Med 1999;31:34 – 45.

3. Martin DC, Fowlkes JL, Babic B, Khokha R. Insulin-like growth factor II signaling in neoplastic proliferation is blocked by transgenic expression of the metalloproteinase inhibitor TIMP-1. J Cell Biol 1999;146:881 – 92.

4. Mira E, Manes S, Lacalle RA, Marquez G, Martinez A. Insulin-like growth factor I-triggered cell migration and invasion are mediated by matrix metalloproteinase-9. Endocrinology 1999;140:1657 – 64.

5. Brown PD. Clinical studies with matrix metalloproteinase inhibitors. APMIS 1999;107:174 – 80.

6. Liotta LA, Steeg PS, Stetler-Stevenson WG. Cancer metastasis and angiogenesis: an imbalance of positive and negative regulation. Cell 1991; 64:327 – 36.

7. Ura H, Bonfil RD, Reich R, et al. Expression of type IV collagenase and procollagen genes and its correlation with the tumorigenic, invasive, and metastatic abilities of oncogene-transformed human bronchial epithelial cells. Cancer Res 1989;49:4615 – 21.

8. Birkedal-Hansen H, Moore WG, Bodden MK, et al. Matrix metalloproteinases: a review. Crit Rev Oral Biol Med 1993;4:197 – 250.

9. Coussens LM, Werb Z. Matrix metalloproteinases and the development of cancer. Chem Biol 1996;3:895 – 904.

10. Waas ET, Lomme RM, DeGroot J, Wobbes T, Hendriks T. Tissue levels of active matrix metalloproteinase-2 and -9 in colorectal cancer. Br J Cancer 2002;86:1876 – 83.

11. Yu AE, Hewitt RE, Kleiner DE, Stetler-Stevenson WG. Molecular regulation of cellular invasion—role of gelatinase A and TIMP-2. Biochem Cell Biol 1996;74:823 – 31.

12. Passlick B, Sienel W, Seen-Hibler R, et al. Overexpression of matrix metalloproteinase 2 predicts unfavorable outcome in early-stage non-small cell lung cancer. Clin Cancer Res 2000;6:3944 – 8.

13. Tokuraku M, Sato H, Murakami S, Okada Y, Watanabe Y, Seiki M. Activation of the precursor of gelatinase A/72 kDa type IV collagenase/ MMP-2 in lung carcinomas correlates with the expression of membrane-type matrix metalloproteinase (MT-MMP) and with lymph node metastasis. Int J Cancer 1995;64:355 – 9.

14. Sato H, Takino T, Okada Y, et al. A matrix metalloproteinase expressed on the surface of invasive tumour cells. Nature 1994;370: 61 – 5.

15. Sato H, Seiki M. Regulatory mechanism of 92 kDa type IV collagenase gene expression which is associated with invasiveness of tumor cells. Oncogene 1993;8:395 – 405.

16. Laack E, Kohler A, Kugler C, et al. Pretreatment serum levels of matrix metalloproteinase-9 and vascular endothelial growth factor in non-small-cell lung cancer. Ann Oncol 2002;13:1550 – 7.

17. Togawa D, Koshino T, Saito T, Takagi T, Machida J. Highly activated matrix metalloproteinase-2 secreted from clones of metastatic lung nodules of nude mice injected with human fibrosarcoma HT1080. Cancer Lett 1999;146:25 – 33.

18. Itoh T, Tanioka M, Matsuda H, et al. Experimental metastasis is suppressed in MMP-9-deficient mice. Clin Exp Metastasis 1999;17:177 – 81.

19. Erlichman C, Adjei AA, Alberts SR, et al. Phase I study of the matrix metalloproteinase inhibitor, BAY 12-9566. Ann Oncol 2001;12: 389 – 95.

20. Rizvi NA, Humphrey JS, Ness EA, et al. A phase I study of oral BMS-275291, a novel nonhydroxamate sheddase-sparing matrix metalloproteinase inhibitor, in patients with advanced or metastatic cancer. Clin Cancer Res 2004;10:1963 – 70.

21. Bertrand JR, Pottier M, Vekris A, Opolon P, Maksimenko A, Malvy C. Comparison of antisense oligonucleotides and siRNAs in cell culture and *in vivo*. Biochem Biophys Res Commun 2002;296:1000 – 4.

22. Aoki Y, Cioca DP, Oidaira H, Kamiya J, Kiyosawa K. RNA interference may be more potent than antisense RNA in human cancer cell lines. Clin Exp Pharmacol Physiol 2003;30:96 – 102.

23. Brummelkamp TR, Bernards R, Agami R. Stable suppression of tumorigenicity by virus-mediated RNA interference. Cancer Cell 2002;2: 243 – 7.

24. Mohan PM, Chintala SK, Mohanam S, et al. Adenovirus-mediated delivery of antisense gene to urokinase-type plasminogen activator receptor suppresses glioma invasion and tumor growth. Cancer Res 1999;59:3369 – 73.

25. Sawaya R, Go Y, Kyritisis AP, et al. Elevated levels of Mr 92,000 type IV collagenase during tumor growth *in vivo*. Biochem Biophys Res Commun 1998;251:632 – 6.

26. Mohanam S, Chandrasekar N, Yanamandra N, et al. Modulation of invasive properties of human glioblastoma cells stably expressing amino-terminal fragment of urokinase-type plasminogen activator. Oncogene 2002;21:7824 – 30.

27. Lakka SS, Gondi CS, Dinh DH, et al. Specific interference of uPAR and MMP-9 gene expression induced by double-stranded RNA results in decreased invasion, tumor growth and angiogenesis in gliomas. J Biol Chem 2005;280:21882 – 92.

28. Jadhav U, Chigurupati S, Lakka SS, Mohanam S. Inhibition of matrix metalloproteinase-9 reduces in vitro invasion and angiogenesis in human microvascular endothelial cells. Int J Oncol 2004;25:1407 – 14.

29. Bridge AJ, Pebernard S, Ducraux A, Nicoulaz AL, Iggo R. Induction of an interferon response by RNAi vectors in mammalian cells. Nat Genet 2003;34:263 – 4.

30. Sledz CA, Holko M, de Veer MJ, Silverman RH, Williams BR. Activation of the interferon system by short-interfering RNAs. Nat Cell Biol 2003;5:834 – 9.

31. Duxbury MS, Matros E, Ito H, Zinner MJ, Ashley SW, Whang EE. Systemic siRNA-mediated gene silencing: a new approach to targeted therapy of cancer. Ann Surg 2004;240:667 – 74.

32. Filleur S, Courtin A, it-Si-Ali S, et al. SiRNA-mediated inhibition of vascular endothelial growth factor severely limits tumor resistance to antiangiogenic thrombospondin-1 and slows tumor vascularization and growth. Cancer Res 2003;63:3919 – 22.

33. Song E, Lee SK, Wang J, et al. RNA interference targeting Fas protects mice from fulminant hepatitis. Nat Med 2003;9:347 – 51.

34. Lee NS, Dohjima T, Bauer G, et al. Expression of small interfering RNAs targeted against HIV-1 rev transcripts in human cells. Nat Biotechnol 2002;20:500 – 5.

35. Lewis DL, Hagstrom JE, Loomis AG, Wolff JA, Herweijer H. Efficient delivery of siRNA for inhibition of gene expression in postnatal mice. Nat Genet 2002;32:107 – 8.

36. McCaffrey AP, Meuse L, Pham TT, Conklin DS, Hannon GJ, Kay MA. RNA interference in adult mice. Nature 2002;418:38 – 9.

37. Ke Z, Lin H, Fan Z, et al. MMP-2 mediates ethanol-induced invasion of mammary epithelial cells over-expressing ErbB2. Int J Cancer 2006;119: 8 – 16.

38. Kinugasa Y, Hatori M, Ito H, Kurihara Y, Ito D, Nagumo M. Inhibition of cyclooxygenase-2 suppresses invasiveness of oral squamous cell carcinoma cell lines via down-regulation of matrix metalloproteinase-2 and CD44. Clin Exp Metastasis 2004;21:737 – 45.

39. Giannelli V, Fontana MR, Giuliani MM, Guangcai D, Rappuoli R, Pizza M. Protease susceptibility and toxicity of heat-labile enterotoxins with a mutation in the active site or in the protease-sensitive loop. Infect Immun 1997;65:331 – 4.

40. Williams TM, Medina F, Badano I, et al. Caveolin-1 gene disruption promotes mammary tumorigenesis and dramatically enhances lung metastasis *in vivo*. Role of Cav-1 in cell invasiveness and matrix metalloproteinase (MMP-2/9) secretion. J Biol Chem 2004;279:51630 – 46.

41. Ray JM, Stetler-Stevenson WG. Gelatinase A activity directly modulates melanoma cell adhesion and spreading. EMBO J 1995;14: 908 – 17.

42. Ray JM, Stetler-Stevenson WG. The role of matrix metalloproteases and their inhibitors in tumour invasion, metastasis and angiogenesis. Eur Respir J 1994;7:2062 – 72.

43. Montgomery AM, Mueller BM, Reisfeld RA, Taylor SM, DeClerck YA. Effect of tissue inhibitor of the matrix metalloproteinases-2 expression on the growth and spontaneous metastasis of a human melanoma cell line. Cancer Res 1994;54:5467 – 73.

44. Elezkurtaj S, Kopitz C, Baker AH, et al. Adenovirus-mediated overexpression of tissue inhibitor of metalloproteinases-1 in the liver: efficient protection against T-cell lymphoma and colon carcinoma metastasis. J Gene Med 2004;6:1228 – 37.

45. Schnaper HW, Barnathan ES, Mazar A, et al. Plasminogen activators augment endothelial cell organization in vitro by two distinct pathways. J Cell Physiol 1995;165:107 – 18.

46. Fang J, Shing Y, Wiederschain D, et al. Matrix metalloproteinase-2 is

required for the switch to the angiogenic phenotype in a tumor model. Proc Natl Acad Sci U S A 2000;97:3884 – 9.

47. Itoh T, Tanioka M, Yoshida H, Yoshioka T, Nishimoto H, Itohara S. Reduced angiogenesis and tumor progression in gelatinase A-deficient mice. Cancer Res 1998;58:1048 – 51.

48. Barasch J, Yang J, Qiao J, et al. Tissue inhibitor of metalloproteinase-2 stimulates mesenchymal growth and regulates epithelial branching during morphogenesis of the rat metanephros. J Clin Invest 1999;103: 1299 – 307.

49. Werb Z, Vu TH, Rinkenberger JL, Coussens LM. Matrix-degrading proteases and angiogenesis during development and tumor formation. APMIS 1999;107:11 – 8.

50. Lara PN, Jr., Stadler WM, Longmate J, et al. A randomized phase II trial of the matrix metalloproteinase inhibitor BMS-275291 in hormone-refractory prostate cancer patients with bone metastases. Clin Cancer Res 2006;12:1556 – 63.

51. Dezube BJ, Krown SE, Lee JY, Bauer KS, Aboulafia DM. Randomized phase II trial of matrix metalloproteinase inhibitor COL-3 in AIDS-related Kaposi's sarcoma: an AIDS Malignancy Consortium Study. J Clin Oncol 2006;24:1389 – 94.

52. Ketting RF, Fischer SE, Bernstein E, Sijen T, Hannon GJ, Plasterk RH. Dicer functions in RNA interference and in synthesis of small RNA involved in developmental timing in C. elegans. Genes Dev 2001;15: 2654 – 9.

53. Dvorak HF. Leaky tumor vessels: consequences for tumor stroma generation and for solid tumor therapy. Prog Clin Biol Res 1990;354A: 317 – 30.

54. Xia H, Mao Q, Paulson HL, Davidson BL. siRNA-mediated gene silencing *in vitro* and *in vivo*. Nat Biotechnol 2002;20:1006 – 10.

55. Vlachaki MT, Hernandez-Garcia A, Ittmann M, et al. Impact of preimmunization on adenoviral vector expression and toxicity in a s.c. mouse cancer model. Mol Ther 2002;6:342 – 8.

Molecular Cancer Therapeutics

Adenovirus-mediated small interfering RNA against matrix metalloproteinase-2 suppresses tumor growth and lung metastasis in mice

Chandramu Chetty, Praveen Bhoopathi, Pushpa Joseph, et al.

Mol Cancer Ther 2006;5:2289-2299.